



## MODELING AND DESIGNING A FULL BEAMFORMER FOR ACOUSTIC SENSING AND MEASUREMENT

A. Lay-Ekuakille<sup>1\*</sup>, N.I. Giannoccaro<sup>2\*</sup>, S. Casciaro<sup>3§</sup>, F. Conversano<sup>4§</sup> and R. Velazquez<sup>5#</sup>

\*Department of Innovation Engineering, University of Salento, 73100, Lecce, Italy

§National Council of Research, Institute of Clinical Physiopathology, 73100, Lecce, Italy

#Faculty of Engineering, Universidad Panamericana, 01001, Aguascalientes, Mexico.

Email: [aime.lay.ekuakille@unisalento.it](mailto:aime.lay.ekuakille@unisalento.it)

*Submitted: June 21, 2017*

*Accepted: July 21, 2017*

*Published: Sep. 1, 2017*

*Abstract - Acoustic sensing is a viable approach for solving issues related to many applications, namely, biomedical, distance measurements, mechanical, health infrastructure monitoring, etc. It is generally sustainable and of no negative impact on the object under test. The use of acoustic sensing under beamforming technique is an important asset to be exploited, especially for the aforementioned applications. This paper illustrates a generalized approach of modeling and designing a full beamformer using two specific classes: LCMP (Linear Constrained Minimum Power) beamformers that are used to overcome robustness limitations and MVDR (Minimum Variance Distortionless Response) beamformers. Any aspect of modeling and designing is always related to the DOA (Direction of Arrival). The obtained results are based on assumptions extracted from an actual case of constructed system.*

**Index terms:** Acoustic sensing, Beamforming, Ultrasonic shape detection, DOA, Distance measurement, array of sensors, interference-to-noise ratio (INR), signal-to-noise ratio (SNR).

### I. INTRODUCTION

Beamforming remains one of the most powerful technique for processing information and signals from an array of sensors or ‘Smart Antenna’ acquiring samples located in a spatial architecture of propagating wave fields. The steering vector of the beamformer is an important aspect since it is used for electrically operating either Uniform Linear Array (ULA) or Uniform Circular Array (UCA) in 2D space [1]. The beamformer linearly combines the

spatially sampled time series from each sensor to obtain a scalar output time series. The goal is to estimate, as accurate as possible, a determined signal coming from a given direction in the space (signal of interest), that is, however, submersed within various interfering signals and noise (Figure1). When the desired signal and the interfering signals simultaneously have the same frequency band [2], it is not certainly possible to exploit the only temporal filtering, to isolate the useful signal [3]. Since the expected signal and interfering ones have usually different origins in spatial regions, this spatial diversity can be used for the aforementioned reason, utilizing a spatial filtering in receiving unit. With beamforming, we indicate a technique by means of which we carry out a versatile form of spatial filtering [4][5][6], to separate signals that are spectrally superposed but that they come from diverse spatial directions [7] [8][9].

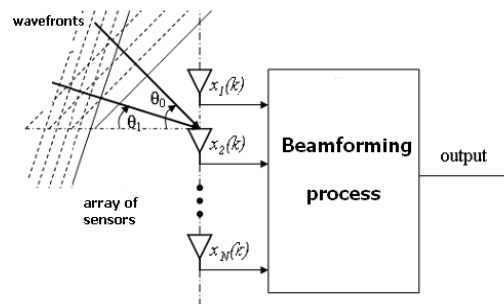


Figure 1. Beamforming process

Let us assume that the incident signal, on the array of sensors, is a complex plane wave, with DOA  $\theta$  and frequency  $\omega$ . Let us take, as reference, the signal of the first sensor with a null phase [10] [11]. This implies that

$$x_1(k) = e^{j\omega k} \quad (1)$$

while

$$x_n(k) = e^{j\omega|k - \Delta_n(\theta)|} \quad (2)$$

for  $2 \leq n \leq N$

The term  $\Delta_n(\theta)$  represents the temporal delay due to propagation between the first sensor and the  $n$ -th one. By replacing Eq.(1) and Eq.(2) at the output [12] of the beamformer, that brings to

$$y(k) = e^{j\omega k} \sum_{n=1}^N w_n^* e^{-j\omega \Delta_n(\theta)} = e^{j\omega k} r(\theta, \omega) \quad (3)$$

$$y(k) = e^{j\omega k} \sum_{n=1}^N \sum_{\xi=0}^{J-1} w_n^* e^{-j\omega[\Delta_n(\theta)+\xi]} = e^{j\omega k} r(\theta, \omega) \quad (4)$$

where, in both cases,  $\Delta_1(\theta)=0$ .

The term  $r(\theta, \omega)$  is the response of beamformer and it could be expressed in vectorial way, as

$$r(\theta, \omega) = w^H d(\theta, \omega) \quad (5)$$

where

$$d(\theta, \omega) = [1 \quad e^{j\omega\tau_2(\theta)} \quad e^{j\omega\tau_3(\theta)} \quad \dots \quad e^{j\omega\tau_D(\theta)}]^H \quad (6)$$

with  $\tau_i(\theta)$ , for  $2 \leq i \leq D$ , corresponding to the temporal delay due to propagation. The vector  $d(\theta, \omega)$  is the response vector of the array also called steering vector or directional vector. Non ideal characteristics of sensors can be included in  $d(\theta, \omega)$ , by multiplying each phase delay by a dedicated function  $a_i(\theta, \omega)$  that describes the response of the related sensor in function of direction and temporal frequency [13]. Hence, it is possible to define the beam pattern [14] as

$$BP = |r(\theta, \omega)|^2 \quad (7)$$

that represents the Energy distribution in the space during transmission step and the direction of major and minor sensitivity during receiving step. A beam pattern is depicted in Fig. 2.

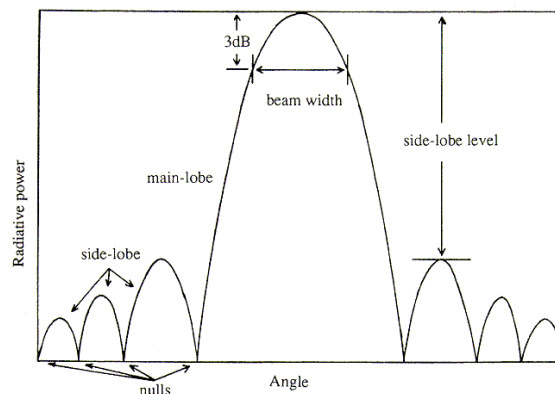


Figure 2. Beam pattern main parameters for a linear array of 8 sensors

Now, let us consider a linear array of sensors; let it  $d$  the reciprocal distance among sensors,  $c$  the propagation speed within the medium and  $\theta$  the DOA of signal [15] with respect to the

versor perpendicular to the direction of the array, see Fig.3 where  $S$  is the source. If we assume that the incident wave is plane, we have

$$\tau_n(\theta) = (n-1) \frac{d}{c} \sin(\theta) \quad (8)$$

and substituting in Eq.(6) we obtain

$$d(\theta, \omega) = \left[ 1 \quad e^{j\omega \frac{d}{c} \sin(\theta)} \quad e^{j\omega 2 \frac{d}{c} \sin(\theta)} \quad \dots \quad e^{j\omega (n-1) \frac{d}{c} \sin(\theta)} \right]^H \quad (9)$$

There are several categories of array of sensors, each one with specific characteristics [16]. This paper, falling within a consolidated research, deals with bi-dimensional arrays since linear arrays are unfit to discriminate the elevation component  $\varphi$  of the DOA; in particular, for sake of simplicity, we have adopted arrays with elements located according to a square array [17].

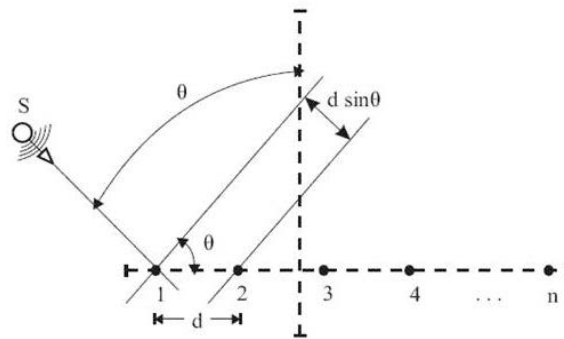


Figure 3. Linear array of  $n$  sensors

The array of sensors, for beamforming considerations, must display some basic characteristics, that is, directivity, array gain versus spatially white noise, and sensitivity and tolerance factor.

## II. PREVIOUS WORK AND ASSUMPTIONS

This paper intends to generalize the modeling and the design of acoustic sensing system based on DOA for objects/obstacles retrieval. Moreover, some specific findings have been included for shape detection and recovery. The research is a follow up of the previous one [18] where a constructed architecture has been tested. The system, as summarized in Figure 4, contains an array of  $n \times m$  ( $n=5, m=5$ ) microphones,  $n$  buffers, an array for signal conditioning, a driving circuit, a beamformer, a dsPIC control, a transmitting circuit based on 555 timer, a ceramic

transducer 328ST160 of Prowave, and a backscattered receiving circuit. A supervising control is acted by means of a dsPIC.

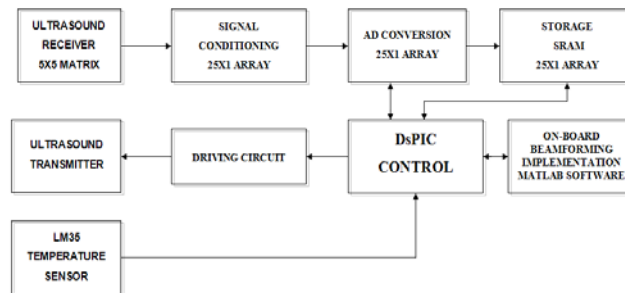


Figure 4. Overall architecture block scheme

For testing the system, the obstacle has been located in an upper position (see Figure5). The time of acquisition is  $t_{stop} - t_{start}$  and the distance  $d$  is calculated by using the well-known formula  $d=ct/2$  in which  $c$  (340 m/s) indicates air wave speed.

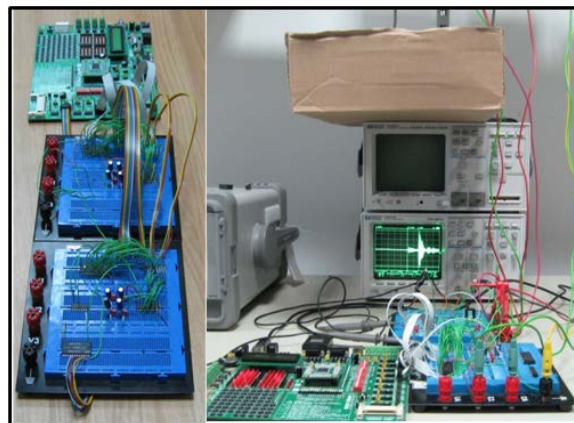


Figure 5. Acoustic sensing system

The system has demonstrated its reliability by performing different measurements within the envisaged distance. Two channels over five have been used to carry out trials.

### III. MODELING AND DESIGNING

The modeling and design mostly concern the application of LCMP and MVDR beamformers for an ideal (Figure 6) and actual array (Figure 7) with 5x5 gridded elements, and separated among them by a distance  $d_x=d_y=\lambda/2$  (see again Figure 6). the frequency at the input of beamformer is 32,8 kHz, equal to the operating frequency of the acoustic transducer while the sound speed to be considered for the simulations is 345 m/s. All simulations are performed for  $n=1000$  samples.

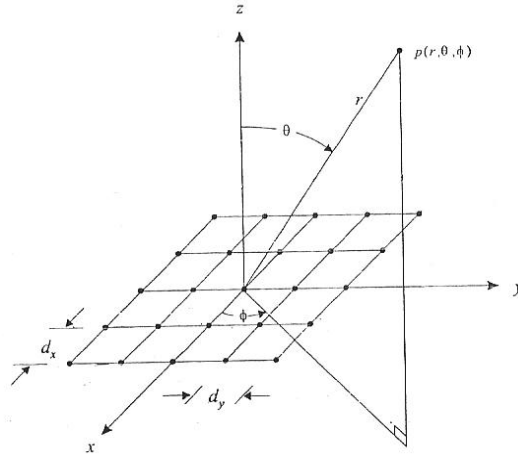


Figure 6. Model of 5x5 array

The main scope of the algorithm for simulation is to minimize the total power at the output of the beamformer related to LCMP and MVDR [19] that is

$$E\{|y|^2\} = E\{w^H XX^H w\} = w^H E\{XX^H\} w = w^H R w \quad (10)$$

with a unity gain ( $w^H d_0 = 1$ ) along the direction of the desired signal  $d_0 = d(\theta_0)$ . That is, we would like to solve the following problem

$$\min_w w^H R w \quad \text{and} \quad w^H d_0 = 1 \quad (11)$$

That is a problem of constrained minimum to be solved with lagrangian multipliers

$$w_{opt} = \min_w [w^H R w + \lambda(w^H d_0 - 1)] \quad (12)$$

The point of the minimum is extracted by setting to zero partial derivatives of the argument of Eq.(12) with respect to  $w$  and  $\lambda$ :

$$\begin{cases} R w + \lambda d_0 = 0 \\ w^H d_0 = 1 \end{cases} \quad (13)$$

that yields to

$$\begin{cases} w = \lambda R^{-1} d_0 \\ \lambda = \frac{1}{d_0^H R^{-1} d_0} \end{cases} \quad (14)$$

hence, obtaining the following solution

$$w = \frac{R^{-1} d_0}{d_0^H R^{-1} d_0} \quad (15)$$

It is necessary to pay attention on the term on the denominator of Eq.(15) that is scalar for simply satisfying the constrain ( $w^H d_0 = 1$ ), in other words to have unity gain along the direction  $\theta_0$ .



Figure 7. Real architecture of a 5x5 array

To implement this algorithm in a real time, it is necessary to apply an adaptive mechanism of estimation of matrix  $R$ . This mechanism is called CLMS (Constrained Least Mean Square) [20]. Instead of minimizing the rms of estimation, we minimize the Lagrangian defined within the problem of optimization according to Eq.(12) as

$$J(w, \lambda) = w^H R w + \lambda^H (w^H d_0 - 1) + \lambda' (w^t d_0^* - 1) \quad (16)$$

where the last term is the conjugate of multipliers of Lagrange, and it is added to force the lagrangian to assume real values. Using  $J(w, \lambda)$  in the relationship of updating weights as

$$C = [d(\theta_0) \quad d(\theta_1) \quad d(\theta_2) \quad \dots \quad d(\theta_L)] \quad (17)$$

we have

$$\begin{aligned} w(k+1) &= w(k) - \mu \nabla_w [w^H R w + \lambda^H (w^H d_0 - 1) + \lambda^H (w^H d_0^* - 1)] \\ &= w(k) - \mu (R w(k) + d_0 \lambda) \end{aligned} \quad (18)$$

The vector  $\lambda$  can be determined imposing that the vector of weights at instant  $k+1$  satisfies the constrain  $w^H(k+1)d_0 = 1$  by obtaining

$$w(k+1) = w(k) - \mu [I - d_0 (d_0^H d_0)^{-1} d_0^H] R w^H + d_0 (d_0^H d_0)^{-1} [1 - w^H d_0] \quad (19)$$

Let us call  $w_c$  the term  $d_0 (d_0^H d_0)^{-1}$  that represents the fixed part of the vector of weights due to the respect of constrains; moreover we can define  $P_a = I - d_0 (d_0^H d_0)^{-1} d_0^H$  as the matrix of projection associated to the adaptive component of the vector of weights. Thanks to the above notations, the equation of the updating of weights becomes

$$w(k+1) = w_c + P_a [w(k) - \mu R w(k)] \quad (20)$$

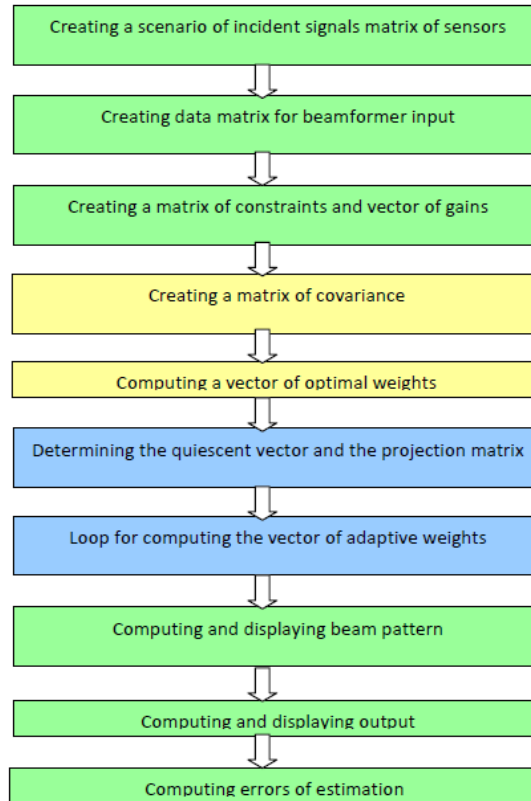


Figure 8. Proposed algorithm for beam pattern and shaping



From Eq.(20) it is now clear the separation between adaptive and non adaptive parts of the vector of weights: the first part depends upon data as input for sensors through the matrix of correlation  $R$ , that is unknown. To make easier the algorithm, we substitute the matrix of correlation with an instantaneous estimation obtained from the scalar product of the vector of data as input ( $X(k)X^H(k)$ ). That is typically done by LMS (least Mean Square). Summarizing, the MVDR in the adaptive version is

$$\begin{aligned}
 P_a &= I - d_0(d_0^H d_0)^{-1} d_0^H \\
 w_c &= d_0(d_0^H d_0)^{-1} \\
 y(k) &= w^H(k)X(k) \\
 w(k+1) &= w_c + P_a[w(k) - \mu y^*(k)X(k)]
 \end{aligned} \tag{21}$$

analogously [19] for LCMP we have a summary of the algorithm as

$$\begin{aligned}
 P_a &= I - C(C^H C)^{-1} C^H \\
 w_c &= C(C^H C)^{-1} \\
 y(k) &= w^H(k)X(k) \\
 w(k+1) &= w_c + P_a[w(k) - \mu X(k)y^*(k)]
 \end{aligned} \tag{22}$$

This algorithm is also expressed, in a concise way, by the flowchart of Figure 8 that describes both MVDR and LCMP beamformers.

#### IV. RESULTS

To make easier the practical application of the algorithm, let us consider the signal of interest arriving, for example, from direction ( $\theta=40$ ,  $\varphi=90$ ) with SNR equal to a 35 dB, and we assume to have three interferences coming from  $DOA_1$  ( $\theta = -60$ ,  $\varphi=40$ ),  $DOA_2$  ( $\theta=-60$ ,  $\varphi=160$ ) and  $DOA_3$  ( $\theta=40$ ,  $\varphi=40$ ) with INR1= 10 dB, INR2= 10 dB and INR3= 10 dB. We assume 0.316 V as a level of background noise, and frequency signal 32.8 kHz and step size  $\mu=10^{-5}$ . We illustrate beam patterns for a 5x5 array of Figure 6, related to MVDR and LCMP, either linear or logarithmic. From Figure 9, we can see that the constrain of unity gain, along

the direction of interest, is satisfied while, from Figure 10, it is possible to appraise the average level of attenuation of side-lobes that is around -15 dB. From Figure 11 that represents the illustration of level curves of the previous beam pattern, we can see the interferences are certainly attenuated, but the beamformer does not impose nulls in correspondence of their directions of arrival: although the directions  $DOA_1 (\theta=-60, \varphi=40)$  and  $DOA_2 (\theta=-60, \varphi=160)$  are located in the vicinity of a zero and are attenuated by more than 70 dB, the direction  $DOA_3 (\theta=40, \varphi=40)$  is somewhat far from the next zero, that leads to an attenuation of 20 dB in that point. The inability to fix nulls along the direction of interferences is a weak point of the MVDR algorithm, that always lowers the ability to estimate the waveform of interest.

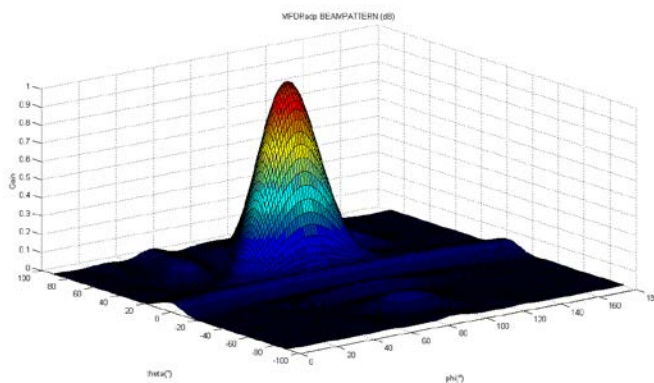


Figure 9. Beam pattern for MVDR case in linear scale

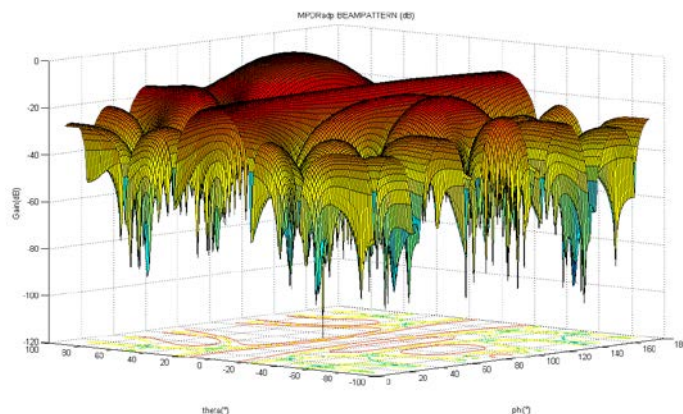


Figure 10. Beam pattern for MVDR case in logarithmic scale

In fact, if, as for the considered case, the output of the beamformer is close to the desired signal (estimation error equal to 1.16%), by increasing the value of INR3 to 40 dB, the output is distorted in a significant way (estimation error equal to 13.63%), as it is demonstrated in Figure 12, where we can see two features of estimated signal, upper, for [35-10-10-10] dB and lower, for [35-10-10-40] dB.

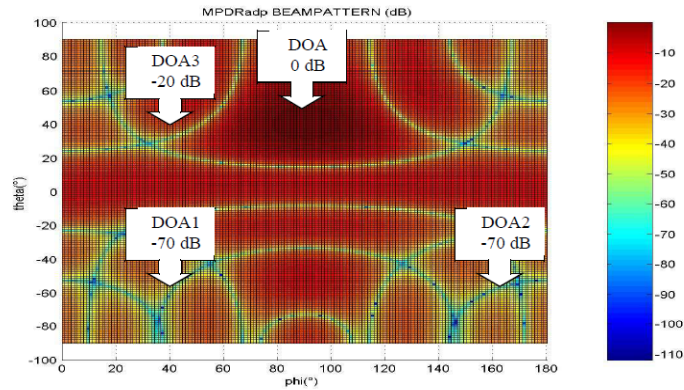


Figure 11. Beam pattern for MVDR in bi-dimensional logarithmic scale

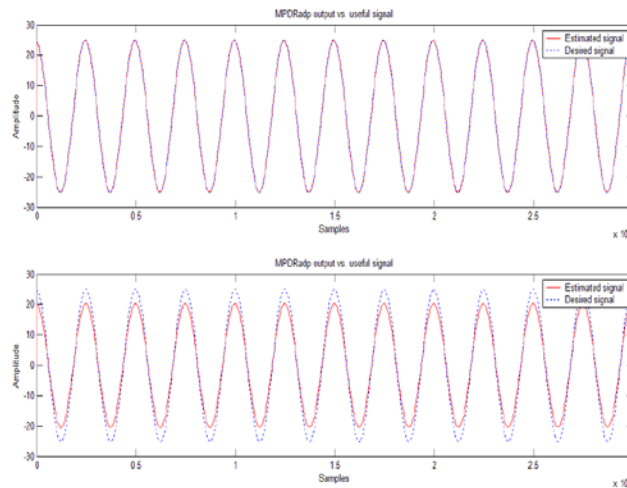


Figure12. Comparison between estimated signal by MVDR beamformer and expected signal for [35-10-10-10] dB (upper) and [35-10-10-40] dB (lower)

To underline the specificity of LCMP with respect to MVDR, it is appropriate to simulate them in the same conditions as it is reported at the beginning of this section. The results are described in Figure 13, Figure14, Figure 15, and Figure 16. LCMP, according to Figure16, does not exhibit a difference, as it is for MVDR (see Figure 12) for [35-10-10-40] dB.

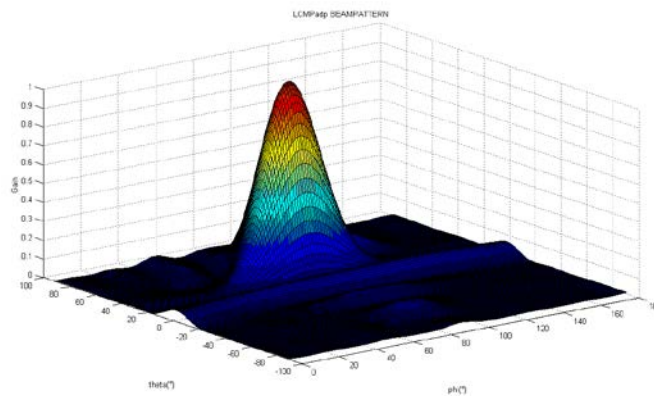


Figure 13. Beam pattern for LCMP case in linear scale

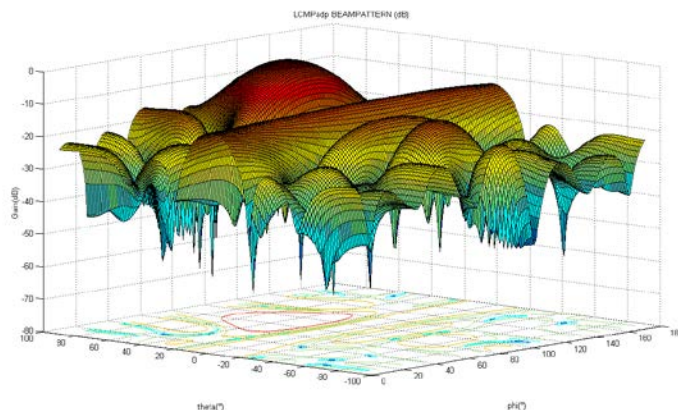


Figure 14. Beam pattern for LCMP case in logarithmic scale

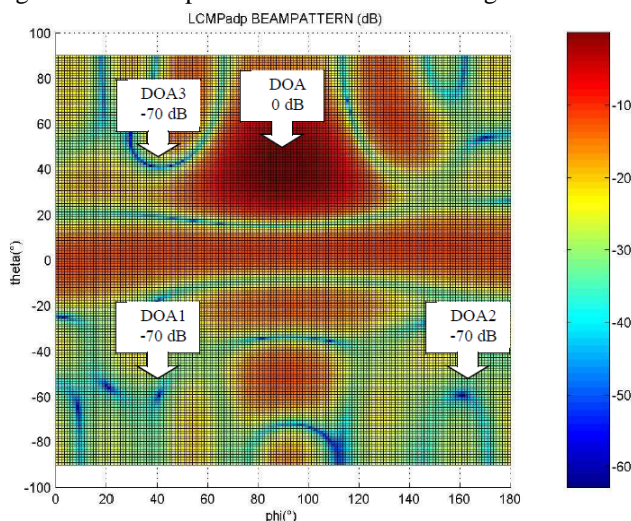


Figure 15 Beam pattern for LCMP in bi-dimensional logarithmic scale

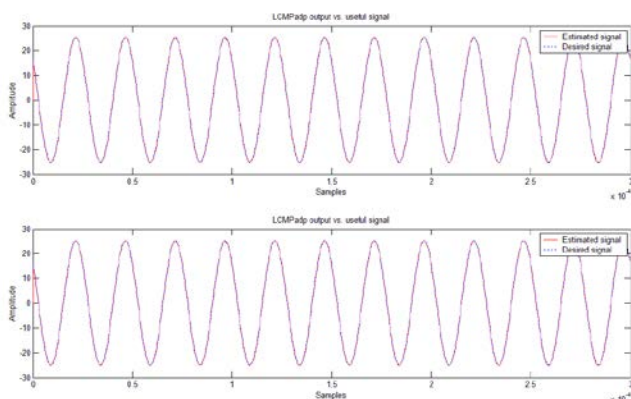


Fig.16 Comparison between estimated signal by LCMP beamformer and expected signal for [35-10-10-10] dB (upper) and [35-10-10-40] dB (lower)

Having illustrated the results of modeling and designing, we are now able to illustrate the effects of the number of sensors of the array with respect to the resolution. Let us adopt a LCMP beamformer since we have already used it before. We have introduced the beam pattern parameters in Figure 2. Let us also introduce another formulation; the beam pattern for an array is defined as the frequency-wavenumber response function assessed versus the

direction [19], that is

$$B(\omega: \theta, \phi) = \gamma(\omega, k) \Big|_{k=\frac{2\pi}{\lambda} a(\theta, \phi)} \quad (23)$$

where  $a(\theta, \phi)$  is a unit vector with spherical coordinate angles. We notice that the beam pattern is the frequency-wavenumber function evaluated on a sphere of radius  $2\pi/\lambda$ . In Eq.(23),  $\gamma(\omega, k)$  is termed as frequency-wavenumber response function of the array of sensor. The 3-dB beamwidth (or the half-power beamwidth, HPBW) is a measure of the width of the beam. It is defined to be the point where  $|B_u(u)|^2 = 0.5$  or  $|B_u(u)| = 1/\sqrt{2}$ . It represents the minimum angular distance that two sources must have, each other, so that they can be distinguished by the beamformer as two distinct sources. The resolution depends upon the geometry of the array and the number of elements; it is very difficult to be determined in analytical way, especially for bi-dimensional arrays. For a  $N \times N$  array of sensors (with  $N=5$ , as for our case), the angular resolution along the directions  $\theta$  and  $\phi$  can be retrieved [21] [22] [23] as

$$HPBW = 2 \arcsin\left(\frac{0.891}{N}\right) \quad (24)$$

With  $N=5$ , the resolution is around  $21^\circ$ , value confirmed by the Figure 17 that represents, with level curves, the linear beam pattern of array up to the value 0.707, that is 3 dB under the maximum value 1.

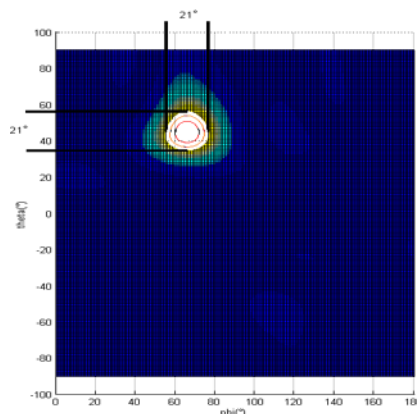


Fig.17 Angular resolution (HPBW) for a 5x5 array of sensors

The angular resolution can be now detailed [24]. Let us consider, for example, the detection of two obstacles in function of  $N$ . Let us also consider three configurations;  $N=5$ ,  $N=8$  and  $N=10$ .

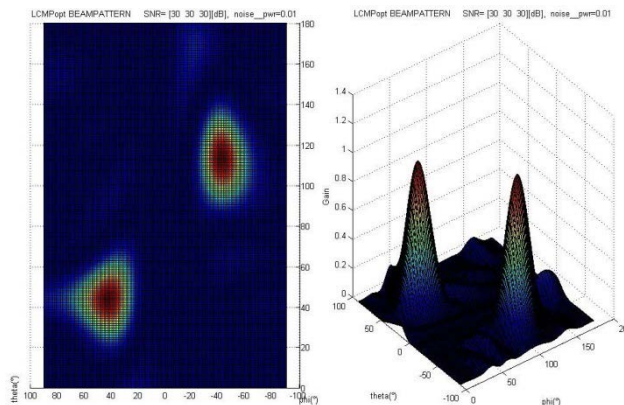


Fig.18 Angular resolution (left) and beam pattern of a 5x5 array of sensors with two detected obstacles.

One can see the improvement of the resolution according to the increasing of the number of the sensors constituting the foreseen array. That is *per se* an expected finding but the best finding is the dimension of the imaging of obstacles depicted by each figure: Figure 18, Figure 19 and Figure 20. There is a strict coincidence between the base aperture (see beam pattern) and the inner dimension of the spot, indicating the resolution, according to imaging located in the left.

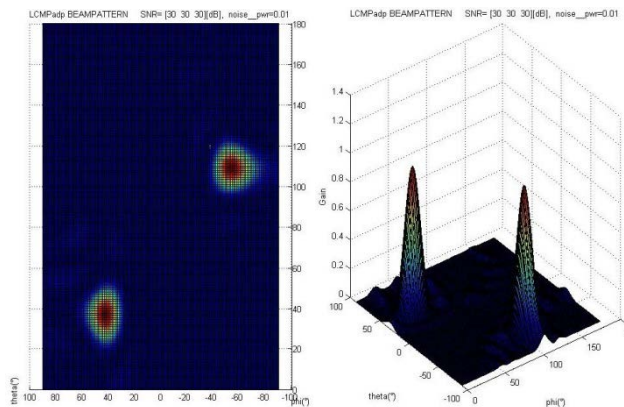


Fig.19 Angular resolution (left) and beam pattern of a 8x8 array of sensors with two detected obstacles.

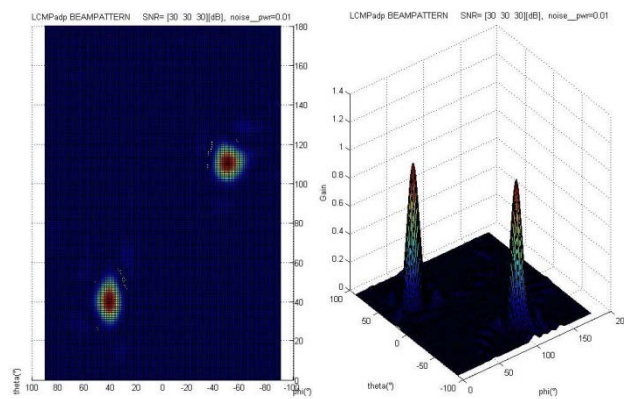


Fig.20 Angular resolution (left) and beam pattern of a 10x10 array of sensors with two detected obstacles.

## V. CONCLUSIONS

Beamforming and array of sensors are intrinsically connected as “siamese children”. Beamforming allows impressive and unexpected use of array of sensors in many fields and applications, namely, biomedical [25] [26], industrial [27], environmental, wireless networking, etc...The main goal of this research, which is still on the way, is to develop applications and new findings in the field of array of sensors using beamforming. This goal also includes a generalization of the approach in order to be able to design and modeling acoustic system. We have demonstrated, thanks to the use of two beamformers, namely, LCMP and MVDR, that it is possible to improve the construction of array of sensors for obstacle detection. It also leads to low cost shaping of objects located at certain distances. The current study, beyond medical ultrasound, is able to lead to material detection and shaping with few sensors, allowing also an imaging fusion [28].

## REFERENCES

- [1] J. Wang, Q. Feng, R. Wu, Z. Su, “A constant-beamwidth beamforming method for acoustic imaging”, Proceedings of IEEE Antennas and Propagation International Symposium, pp. 4236-4239, 2007, Honolulu, USA.
- [2] B.D. Van Veen, K.M. Buckley, Beamforming: “A versatile approach to spatial filtering”, IEEE ASSP Magazine, vol. 5, no.2, pp.4-24, 1988
- [3] G. Okamoto, “Jammer nulling via low complexity blind beamforming algorithm”, Proceedings IEEE Antennas and Propagation International Symposium, pp. 25-28, 2007, Honolulu, USA.
- [4] O.L. Frost III, “An algorithm for Linearly Constrained Adaptive Array Processing”, Proceedings of IEEE, vol. 60, pp.926-935, August 1972.
- [5] A. Lay-Ekuakille, A. Trotta, G. Vendramin, “Beamforming based acoustic imaging for distance retrieval”, Proceedings of IEEE I2MTC, pp. 1466-1470 2008, Victoria, Vancouver Island, Canada.
- [6] E. Warsitz and R. Haeb-Umbach, “Acoustic filter-and-sum beamforming by adaptive principal component analysis”, Proceedings of IEEE ICASSP, pp. 797-800, 2005, Philadelphia, USA.
- [7] G. Soloperto, F. Conversano, A. Greco, E. Casciaro, A. Ragusa, S. Leporatti, A. Lay-Ekuakille, S. Casciaro, “Multiparametric Evaluation of the Acoustic Behaviour of

- Halloysite Nanotubes for Medical Echographic Image Enhancement”, IEEE Transactions on Instrumentation & Measurement, vol. 63, no.6, pp. 1423 – 1430, 2014,
- [8] S. Casciaro, F. Conversano, P. Pisani, A. Greco, A. Lay-Ekuakille, M. Muratore, “A New Ultrasound Parameter for Osteoporosis Diagnosis: Clinical Validation on Normal- and Under-Weight Women “, Proceedings of IEEE MeMea 2015, pp. 250-254, 2015, Turin, Italy
- [9] R.O. Schmidt, “Multiple emitter location and Signal parameter estimation”, Proceedings of RADC Spectrum Estimation Workshop, pp.243-258, Griffiths AFB, Rome, New York, 1979.
- [10] R.O. Schimidt, Multiple emitter location and signal parameter estimation, in Proc. of RADC Special Estimation Workshop, pp.243-258, Griffiths AFB, New York, , Reprinted in IEEE Trans.AP-34, pp.276-280, 1986
- [11] H. Krim and M. Viberg, “Two decades of array signal processing research: The parametric approach “, IEEE Signal Processing Magazine, vol.13, pp 67-94, 1996.
- [12] A. Margarita, S.J. Flores, L. Rubio, V. Almenar, J.L. Corral, “Application of MUSIC for spatial reference beamforming for SDMA in a smart antenna for GSM and DECT”, Vehicular Technology Conference, pp. 123-126, 2001.
- [13] N.I. Giannoccaro, A. Massaro, L. Spedicato and A. Lay-Ekuakille, “Detection Analysis of Small Notches Damages Using a New Tactile Optical Device”, IEEE/ASME Transactions on Mechatronics, vol. 20, no.1, pp.313-320, 2015.
- [14] Y. Rockah and P.M. Schultheiss, “Array shape calibration using sources in unknown locations-part II: Near-field sources and estimator implementation”, IEEE Trans. Acoust.,Speech, Signal process, vol.35, no.6, pp.724-735, 1987.
- [15] P. Vergallo, A. Lay-Ekuakille, “Brain Source Localization: A New Method Based on Music Algorithm and Spatial Sparsity”, Rev. Sci. Instrum. 84, 085117-085123, 2013.
- [16] K.L. Bell, H.L. Van Trees, “Adaptive Beamforming for Spatially Spread Sources”, Proceedings of IEEE Signal Processing Workshop, pp. 1-4, 1998.
- [17] A. Lay-Ekuakille, G. Vendramin, A. Trotta, “Acoustic Sensing for Safety Automotive Applications”, Proceedings of the 2nd International Conference on Sensing Technology, pp. 1-7, 2007 Palmerston North, New Zealand.
- [18] A. Lay-Ekuakille, P. Vergallo, D. Saracino, A. Trotta, “Optimizing and Post Processing of a Smart Beamformer for Obstacle Retrieval”, IEEE Sensors Journal, vol.12, no. 5, pp.1294-1299, 2012



- [19] H. Van Trees, "Optimum Array Processing (Part IV): Detection, Estimation, and Modulation Theory", Wiley Interscience, New York, 2002
- [20] J. J. Fuchs, "Linear programming in spectral estimation: Application to array processing," Proceedings of IEEE International Conference on Acoustics, Speech, and Signal Processing, vol. 6, pp. 3161–3164, 1996
- [21] J. J. Fuchs, "On the application of the global matched filter to DOA estimation with uniform circular arrays," IEEE Trans. Signal Processing, vol. 49, no. 4, pp. 702–709, 2001.
- [22] A. Lay-Ekuakille., C. Pariset, A. Trotta, "FDM-based Leak Detection of Complex Pipelines: Robust Technique for Eigenvalues Assessment", Measurements Science Technology, Vol.21, no.11, pp.1-8, 2010
- [23] N. I. Giannoccaro, L. Spedicato , A. Messina, A. Lay-Ekuakille, "Ultrasonic visibility tests and estimation of specular target plane orientation through a robotic scanning", Proceedings of IEEE SSD 2014, pp.1-6, 2014, Castelldefels-Barcelona, Spain
- [24] P. Vergallo, A. Lay-Ekuakille, D. Caratelli, "Sparsity of the Field Signal-Based Method for Improving Spatial Resolution in Antenna Sensor Array Processing", Progress in Electromagnetics Research – PIER, vol.142, pp.369-388, 2013
- [25] G. Soloperto, F. Conversano, E. Casciaro, A. Greco, G. Gigli, A. Lay-Ekuakille, S. Casciaro, "Laser Fluence and Exposure Time Effects on Optoacoustic Signal from Gold Nanorods for Enhanced Medical Imaging", Proceedings of IEEE I2MTC 2014, pp.1139-1143, 2014, Montevideo, Uruguay.
- [26] S. Casciaro, P. Pisani, G. Soloperto, A. Greco, A. Lay-Ekuakille, F. Conversano, "An Innovative Ultrasound Signal Processing Technique to Selectively Detect Nanosized Contrast Agents in Echographic Images", IEEE Transactions on Instrumentation & Measurement, vol. 64, no.8, pp. 2136-2145, 2015,
- [27] M.G. De Giorgi, A. Ficarella, A. Lay-Ekuakille, "Monitoring Cavitation Regime from Pressure and Optical Sensors: Comparing Methods using Wavelet Decomposition for Signal Processing", IEEE Sensors Journal, vol.15, no.8, pp. 4684-4691, 2015
- [28] V. Bhateja, H. Patel, A. Krishin, A. Sahu, A. Lay-Ekuakille, "Multimodal Medical Image Sensor Fusion Framework Using Cascade of Wavelet and Counterlet Transform Domains", IEEE Sensors Journal, vol.15, no.12, pp.3783-3790, 2015